Applications of midinfrared quantum cascade lasers to spectroscopy

Gus Hancock
Grant Ritchie
Jean-Pierre van Helden
Richard Walker
The University of Oxford
Department of Chemistry
The Physical and Theoretical Chemistry Laboratory
South Parks Road
Oxford, OX1 3QZ, United Kingdom
E-mail: grant.ritchie@chem.ox.ac.uk

Damien Weidmann
The University of Oxford
Department of Chemistry
The Physical and Theoretical Chemistry Laboratory
South Parks Road
Oxford, OX1 3QZ, United Kingdom
and
STFC Rutherford Appleton Laboratory
Space Science & Technology Department
Harwell Science and Innovation Campus
Didcot, OX11 0QX, United Kingdom

Abstract. We review the use of both pulsed and continuous wave quantum cascade lasers in high-resolution spectroscopic studies of gas phase species. In particular, the application of pulsed systems for probing kinetic processes and the inherent rapid passage structure that accompanies observations of low-pressure samples using these rapidly chirped devices are highlighted. Broadband absorber spectroscopy and time-resolved concentration measurements of short-lived species, respectively exploiting the wide intrapulse tuning range and the pulse temporal resolution, are also mentioned. For comparison, we also present recent sub-Doppler Lamb-dip measurements on a low-pressure sample of NO, using a continuous wave external cavity quantum cascade laser system. Using this methodology the stability and resolution of this source is quantified. We find that the laser linewidth as measured via the Lamb-dip is ca. 2.7 MHz as the laser is tuned at comparably slow rates, but decreases to 1.3 MHz as the laser scan rate is increased such that the transition is observed at 30 kHz. Using this source, wavelength modulation spectroscopy of NO is presented. © *2010 Society of Photo-Optical Instrumentation Engineers.* [DOI: 10.1117/1.3498770]

Subject terms: quantum cascade laser; rapid passage; modulation spectroscopy; Lamb-dip; midinfrared; reaction kinetics.

Paper 100328SSR received Apr. 14, 2010; revised manuscript received Jun. 23, 2010; accepted for publication Jun. 24, 2010; published online Nov. 22, 2010.

1 Introduction

Quantum cascade lasers (QCLs) are rapidly becoming the radiation source of choice for practitioners working within the midinfrared (mid-IR) (4 to 14 μm) and at longer wavelengths. The devices, whether pulsed or continuous, offer high output power, room temperature operation, single-mode character, and wide tunability, making them ideal tools for high-resolution spectroscopy with a wide variety of applications. Recent work has seen the application of QCLs to breath analysis, atmospheric sensing, plasma spectroscopy, and reaction kinetics.[1–12] These devices are progressively taking over the mid-IR laser market and will continue to do so as their reliability, output power, wall plug efficiency, and tunability continue to improve, and their emission wavelengths decrease toward the 3-μm region where many molecules have strong C—H, N—H, and O—H stretching vibrations. In this paper, we discuss some applications of these devices for measurements of interest to gas phase kinetics and nonlinear spectroscopy, which are enabled by the high chirp rate and high output power of mid-IR QCLs.

2 QCLs Operated in the Pulsed Mode

2.1 *Rapid Passage Effect*

The majority of QCL-based studies that have been conducted have employed pulsed sources in which Joule heating leads to rapid changes in the optical length of the laser cavity and hence the laser frequency towards lower frequencies, i.e. the laser output is chirped. The chirp rate is often of the order of 10^{-3} cm^{-1} ns^{-1}, as can be seen from the spectrum shown in Fig. 1, and directly impacts on the spectral resolution of spectrometers based on pulsed QCLs. This limitation has been described in the literature,[3,13] where the spectral resolution $\Delta\nu$ is given by

$$\Delta\nu = \left(C\frac{\mathrm{d}\nu}{\mathrm{d}t}\right)^{1/2}, \tag{1}$$

where $\mathrm{d}\nu/\mathrm{d}t$ is the chirp rate of the QCL, and C is a constant depending on the characteristics of the acquisition system. The chirp rate is not constant across the duration of the applied current pulse and therefore neither is the spectral resolution.

In addition to this instrumental linewidth, which is often larger than the contribution due to Doppler broadening, the use of chirped radiation to probe samples at reduced pressure leads to measured spectral lines that are not symmetric, as would be observed in conventional absorption spectroscopy, but displaying both absorptive and emission components, as depicted in Figs. 1 and 2. This is due to the rapid passage (RP) effect, where the laser frequency is chirped through the molecular resonance on a timescale that is short compared to the time between collisions; as such, the sample is polarized and it is the interference between this induced polarization and the chirped laser radiation field that results in the observed signal.[3,14–16] The RP effect, however, can be removed by increasing the overall pressure by the introduction of an inert buffer gas, typically of the order of 100 Torr, such that the collision rate is increased and the sample polarization and/or coherence is destroyed on a timescale shorter than that of the signal acquisition system.[12] An example of such behavior is shown in Fig. 2.

0091-3286/2010/$25.00 © 2010 SPIE

Downloaded from SPIE Digital Library on 26 Nov 2010 to 130.246.132.178. Terms of Use: http://spiedl.org/terms

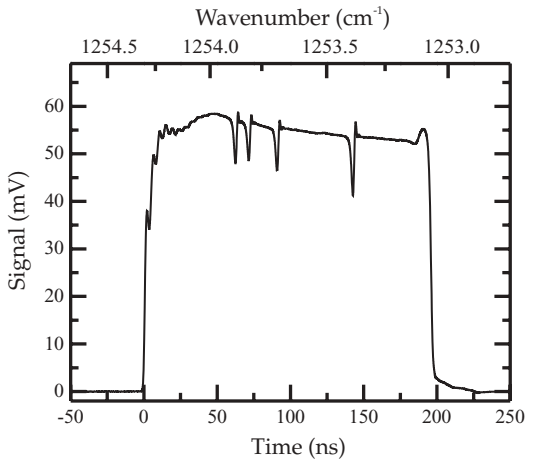

Fig. 1 Raw intra pulse spectrum of 130 mTorr of methane in a 40-cm path length, showing *P*(8) and *P*(9) transitions in the fundamental band of the triply degenerate ν_4 bending vibration in the range 1253 to 1254 cm^{-1}.

A pulsed distributed feedback (DFB) QCL (Alpes Laser) housed and driven by a Q-MACS system from Neoplas Control, operating in the intrapulse mode (see later) was utilized. A single current pulse of 190 ns length was applied to the chip, and current detuning occurred between 1253.3 and 1254.2 cm^{-1} during this period, with a chirp rate varying between 225 and 160 MHz ns^{-1}, producing an average pulse power of ca. 20 mW. The radiation was directed through a 40-cm-long cell containing 130 mTorr of CH_4 and onto a thermoelectrically cooled mercury cadmium telluride detector (VIGO PVI-2TE-10.6) with a fast preamplifier (Neoplas control). The resulting data were recorded on a 2 Gsample/s 350-MHz bandwidth digital oscilloscope (LeCroy Wavesurfer 434). At low pressure, the characteristic oscillation between absorption and emission signals associated with rapid passage is readily apparent. When the pressure, and hence the collision rate, is increased by the introduction of 100 Torr of a buffer gas (Ar), however, the interference effects are washed out and the spectral line shape becomes a Voigt, as one would expect for traditional direct absorption spectroscopy. Note that under these higher pressure conditions, both the number density and the linewidth match the expected values.[12] The rapid passage, however, does little to affect the sensitivity of the system, and for the unbuffered data, a sensitivity of 1.2×10^{-5} cm^{-1} $Hz^{-1/2}$ was achieved in 5000 averages, something that could likely be improved by an order of magnitude by pulse normalization.[17,18]

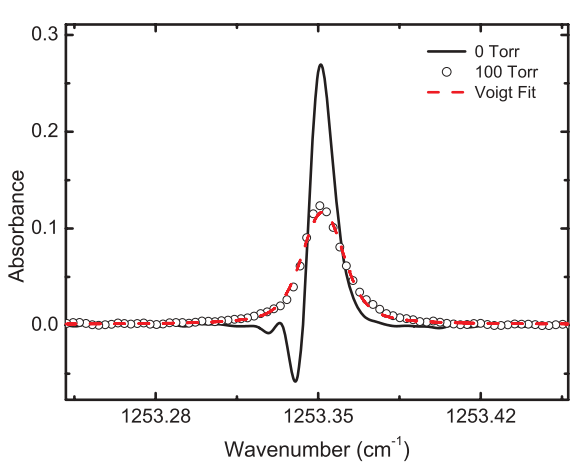

Fig. 2 Spectrum of the *P*(8) transition in the fundamental ν_4 band of CH_4 showing 130 mTorr of CH_4 with and without the addition of 100 torr buffering Ar gas. The high pressure data is shown overlaid with a Voigt fit showing the return to 'normal' behaviour at this pressure.

The standard method for modeling RP signals is via the optical Bloch equations in which both the real and imaginary parts of the complex refractive index and the associated population transfer are calculated as the rapidly swept radiation field interacts with the (simplified) two-level system.[19] Correct implementation of the optical Bloch equations requires knowledge of both the population and polarization decay rates; in gas phase studies, it is common to make the approximation that these two rates are very similar, and equal to the rate of collisional relaxation. However, detailed measurements of RP effects and how they are affected by the presence of different perturbers clearly indicate that this assumption is too simplistic and that this form of coherent spectroscopy can provide intriguing insights into the roles of elastic and inelastic collisions and any velocity-dependent effects.[20]

2.2 *Broadband Absorber Spectroscopy*

Pulsed QCLs are traditionally used in two modes of operation: the interpulse and the intrapulse. The first of these seeks to minimize the effects of the inherent frequency chirp by utilizing current pulses of the order of <20 ns and often using relatively high pressure samples. The frequency tuning is then achieved by adding a subthreshold low-frequency current ramp to the pulse train. Conversely, the intrapulse method embraces the frequency chirp and seeks to lengthen the current pulse so that as wide a range of frequencies as possible can be probed in a single pulse; in this mode, a range of ca. 1 to 2 cm^{-1} can be covered using a 0.2- to 2-μs-long pulse. The length of pulse is usually limited by the gain and/or temperature dissipation of the QCL chip, and often under the conditions of a longer pulse (>500 ns), the final laser output power has diminished by 60 to 70% from that at the beginning of the pulse. Also, as the temperature changes, so does the rate of heating, and toward the end of the pulse, the chirp rate can be as low as a few megahertz per nanosecond, providing an increased spectral resolution.

As mentioned, the intrapulse method enables a relatively wide wave number range to be accessed, and this can often provide sufficient spectral range over which one can unambiguously identify relatively "large" molecules whose IR spectra exhibit broadband features and are not rotationally resolved. Figure 3 shows an example of such a case for the molecule isoprene C_5H_8 for excitation of its out of plane (C–H) wagging vibration around 10 μm (Ref. 21). The same cell and detection system were utilized as for the CH_4 work, but now in combination with a prototype laser developed by J. Cockburn's group at the University of Sheffield, United Kingdom. Current pulses of 500 ns were applied to the gain medium at a rate of 5 kHz and light was emitted between 991.3 and 992.5 cm^{-1} during this time with a chirp rate in the range 50 to 100 MHz ns^{-1}. Note that even in the case of this rotationally unresolved spectrum, the effects of RP can be clearly seen with a number of asymmetric line shapes superimposed on a continuous background, and once again, addition of some buffer gas removes this effect.

Downloaded from SPIE Digital Library on 26 Nov 2010 to 130.246.132.178. Terms of Use: http://spiedl.org/terms

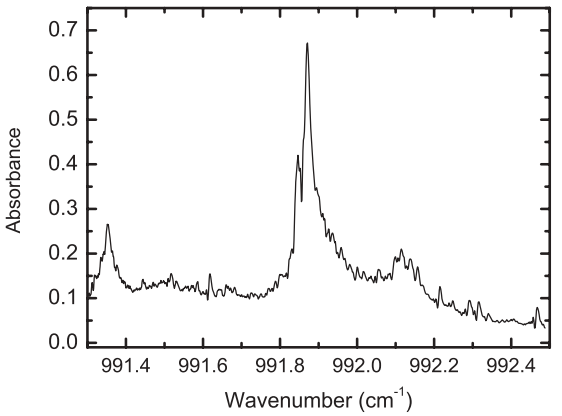

Fig. 3 Typical intrapulse spectrum of isoprene obtained around 10 μm. Despite the lack of rotationally resolved features, RP structures are still evident in the low-pressure spectrum.

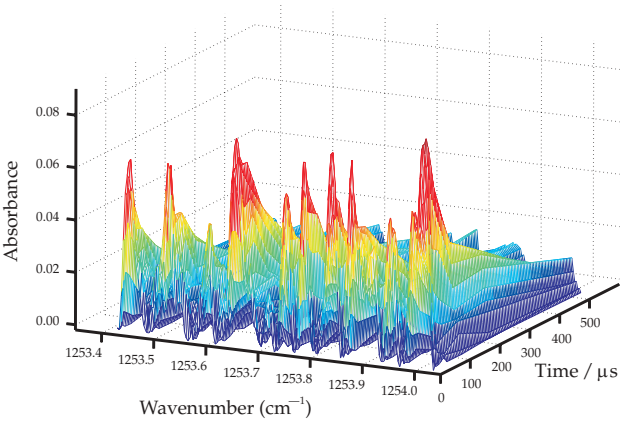

Fig. 4 Evolution of the IR spectrum of CF_3 between 1253.4 and 1254.0 cm^{-1}, as a function of time after the 266-nm photolysis event. The time-dependent absorption enables the CF_3 radical recombination rate constant to be determined.

2.3 *Time-Resolved Measurements of Radical Concentrations*

One suitable application of these pulsed devices is in monitoring time-dependent processes such as in studies of reaction kinetics and dynamics, and of ignition and perturbations in plasma and combustion systems. In such cases, concentrations may change on timescales of the order of 0.1 to 10 μs. We have, for example, demonstrated the use of a pulsed QCL to study the kinetics of a photolysis event, and the ensuing molecular reaction.

The 8-μm output from the source previously mentioned was spatially overlapped with a counterpropagating 266-nm Nd:YAG laser (Spectra Physics LAB-130) through a 50-cm-long cell with CaF_2 windows. The simplistic and easy controllable nature of the acquisition process in intrapulse mode enables a complete spectrum to be measured on a timescale conducive to monitoring both nascent and relaxing fragment concentrations, and thus the concentration and energy distribution of CF_3 radicals produced from the photolysis of CF_3I could be determined.[11] The CF_3 radical concentration was recorded as a function of delay between photolysis and probe pulses, and the CF_3 radical concentration resolved over several hundred microseconds, and radical recombination was observed. An example of typical data obtained is shown in Fig. 4, as the CF_3 spectrum at 1253.4 to 1254.0 cm^{-1} evolves over time following the initial photolysis pulse. Once analyzed and matched to the reaction scheme, the returned radical-radical recombination rate constant for the formation of C_2F_6 was found to 3.9×10^{-12} cm^3 $molecule^{-1}$ s^{-1}, in excellent agreement with previous literature values.[22–25]

3 QCLs Operated in the cw Mode

3.1 *Lamb-Dip Spectroscopy*

Development of more efficient QCL structures has meant that high-power (>100 mW) continuous wave (cw) single-mode operation is now routinely achievable at room-temperature. Therefore the resolution of room-temperature QCL absorption spectrometers are no longer dominated by the fast frequency chirp inherent to pulsed operation, and as such high-resolution spectroscopy can now be undertaken with far less complex systems. In addition, the development of broadband QCL structures to be used as the gain medium in external cavity systems has led[26,27] to increasingly wide tuning ranges (>15% of the central frequency). The cw external cavity QCLs sources (EC-QCL) are commercially available (Daylight Solutions) and the spectroscopic studies presented here were obtained with a system reaching over 190 cm^{-1}, with a central frequency of 5.35 μm. Larger tuning ranges have been reported in the literature[28–30] and through the combination of multiple-cascade QCL structures, EC sources with tuning ranges up to 430 cm^{-1} have been demonstrated.[31] In addition to high-resolution studies[32] on NO and DBr around 5.3 μm (Ref. 33), the high output power of the EC-QCL source has been exploited to investigate nonlinear effects.

For example, measuring the Lamb-dip width provides a good estimate of the free-running laser linewidth of the EC-QCL, as well as its evolution in various frequency tuning schemes. Figure 5(a) shows an example of the Lamb-dip spectra observed when the EC-QCL beam propagates through a 70-cm-long cell containing a low pressure of NO, is retroreflected with a mirror, and directed onto a MCT detector (VIGO PVI-2TE-6). The two spectral lines shown probe both Λ-doublets (e,f) of the $v=0, J=13.5$, state on the $R(13.5)_{1/2}$ transition around 1920.7 cm^{-1}. The laser frequency is swept through the wave number range at a frequency of 40 Hz by applying a voltage to the piezoelectric transducer controlling the external cavity grating. The (nearly) counterpropagating beams are aligned such that feedback into the EC-QCL, which will cause frequency and amplitude instabilities, is minimized.

The data plotted in Fig. 5 were obtained by averaging 80 individual scans. As the laser frequency fluctuations, due to both mechanical stability of the cavity and low-frequency noise in the current controller, were too large to enable observation of individual Lamb-dips using scope-based averaging, the 80 individual scans were postprocessed, recentered, and then the averaging was performed. The experiment was carried out under the following conditions: a laser output power of 160 mW as the "pump" beam, a beam waist of 0.6 mm, a NO partial pressure of 37 mTorr, and a residual air pressure of 38 mTorr.

Downloaded from SPIE Digital Library on 26 Nov 2010 to 130.246.132.178. Terms of Use: http://spiedl.org/terms

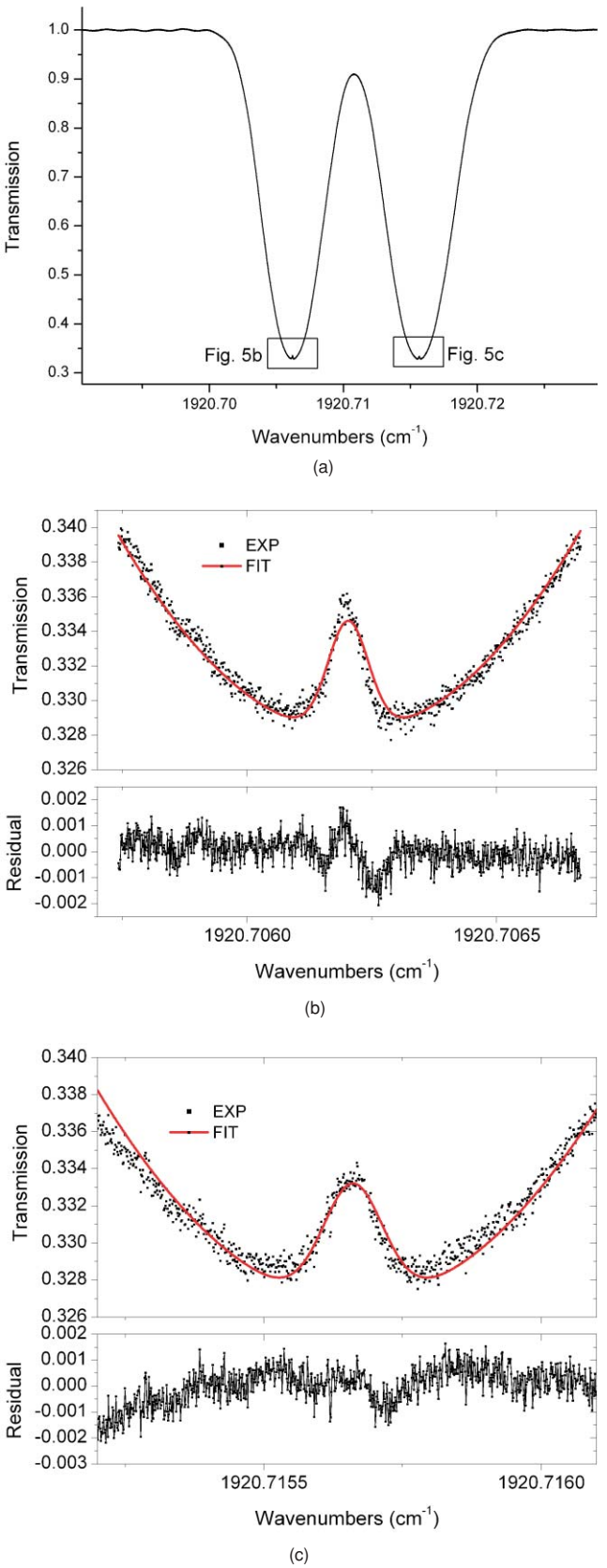

Fig. 5 (a) Lamb-dip signals produced from 37 mTorr of NO in a 70-cm-long cell and probing both Λ doublets of $v = 0$, $J = 13.5$ within the $^2\Pi_{1/2}$ spin-orbit state on the $R(13.5)$ transition and (b) and (c) close-ups on the Lamb dips of both transitions and corresponding global fits and residuals. Experimental data, points, fitted model, solid line; and residual (lower panel) values.

Following Demtröder's[34] formalism, the saturation parameter S (applicable to strong laser fields) is given by

$$S = \frac{2I_p\mu^2\tau_t^2}{\varepsilon_0 ch^2}, \tag{2}$$

where μ is the transition dipole moment, I_p is the pump intensity, τ_t is the transit time, ε_0 is the permittivity of free space, c is the speed of light, and h is Planck's constant. The lineshape $\alpha(\omega)$ accounting for the Lamb-dip is then given as a function of the unsaturated Doppler line shape $\alpha_D(\omega)$ by

$$\alpha(\omega) = \alpha_D(\omega)\frac{\Gamma}{B(\omega)\{1-[2(\omega-\omega_0)/A(\omega)+B(\omega)]^2\}^{1/2}}, \tag{3}$$

with

$$A(\omega) = \sqrt{[(\omega-\omega_0)^2+\Gamma^2]}^{1/2}$$

and

$$B(\omega) = \sqrt{[(\omega-\omega_0)^2+(1+2S)\Gamma^2]}^{1/2}$$

where $(\omega - \omega_0)$ is the frequency detuning from line center, Γ is the homogeneous half width given by the root mean square sum of the transit time broadening and the collisional broadening, and was calculated to be 240 kHz. Using this model, the theoretical transmission spectra were generated and then convoluted with a Gaussian line shape to account for the effective laser linewidth. Since the homogenous broadening is much smaller than the laser linewidth, the experimentally observed Lamb-dip widths are a direct measurement of the laser linewidth. The Lamb-dip spectra observed on the Λ doublet-resolved transitions appearing in Fig. 5(a) were fit in a global routine, as is seen in Fig. 5(b) and 5(c) and widths of 2.4 and 3.2 MHz were returned for the lower and higher wave number transitions, respectively, with an average transition dipole moment of 2.3×10^{-3} D. Similarly, Gaussian profiles fitted directly to the Lamb-dips returned widths of 2.3 ± 0.1 and 3.1 ± 0.1 MHz, respectively. Both the transition dipole moments and laser bandwidth-dominated linewidths are in reasonable agreement with those in the literature,[35–37] and discrepancies between values are likely due to nonlinearities in the scanning frequency.

That the Lamb-dip is best modeled by a Gaussian profile is a result mirrored in the literature,[35,36,38] and is most likely due to injection current fluctuations. Investigation on the influence of the frequency scan rate on the observed laser linewidth has confirmed this. In this case, the frequency tuning rate was increased by application of a sine wave modulation to the injection current of the QCL, and Lamb-dips measured using the methodology presented earlier with the substitution of a faster detector (VIGO PVI-2TE-10.6). Even though the QCL bias tee and the acquisition electronics limit the range of accessible scan rates to between 5 kHz and 2 MHz, a general linear decrease in laser linewidth was observed, down to 1.3 MHz at 30 kHz, when our detector bandwidth became the limiting factor. While the averaging process effectively lengthens the measurement time, and thus would allow more laser jitter to affect the results, the measured Lamb-dip widths for both single shot and averaged data gave essentially identical values. Thus, averaged data, which has a lower uncertainty due to a higher SNR was determined appropriate for use. Extrapolating the measured values for the linewidth obtained at kilohertz scan rates to

Downloaded from SPIE Digital Library on 26 Nov 2010 to 130.246.132.178. Terms of Use: http://spiedl.org/terms

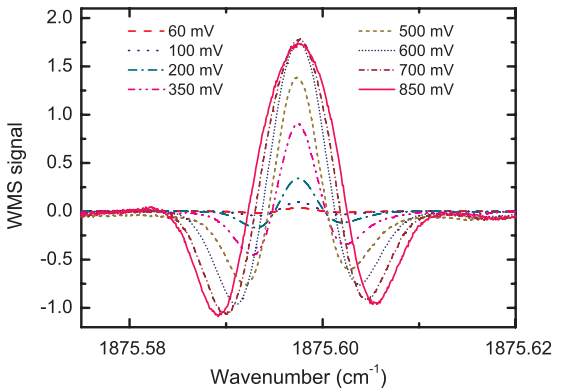

Fig. 6 Second-harmonic WMS spectra of the $Q(3.5)$ Λ-doublet of NO within the $^2\Pi_{3/2}$ spin-orbit state at 1875.59 cm^{-1} as a function of applied modulation voltage. Here 1 mV corresponds to a 0.2-MHz modulation amplitude.

dc gives a linewidth value of ca. 2.5 MHz. This is consistent with our "slow" tuned measurements obtained through external cavity mechanical modulation and reflects the increase in measured linewidth when the transition was scanned over a longer time period. Note also that in this case, the accessible scan range was far less than at the lower scan rates and the measurements were frequency calibrated using the width of one of the Λ doublet transitions. The low-frequency jitter cancellation methodology already mentioned also enabled the analysis of the variation in the measured separation of the Lamb-dips on this pair of transitions, and we could deduce the tuning stability of the system, returning a deviation of about 3% from the expected value of 277 MHz as given[39] in HITRAN.

3.2 *Wavelength-Modulation Spectroscopy*

All of the sensitivity-enhancing techniques that have previously been employed for absorption studies using telecom diode lasers can be adapted to QCL spectroscopy and the literature contains many examples such as noise-immune cavity-enhanced optical heterodyne molecular spectroscopy[40] (NICE-OHMS), photoacoustic spectroscopy,[41] and Faraday rotation spectroscopy.[42] Perhaps the most straightforward methodology is wavelength modulation spectroscopy (WMS), which can be readily achieved by modulating either the external cavity or the injection current of the EC-QCL. Figure 6 shows typical WMS signals obtainable with a low pressure Doppler broadened sample of NO and modulation of the laser injection current at a frequency of 15 kHz. A 5-cm-long cell with CaF_2 windows was utilized, containing 140 mTorr of NO, and the e and f components of the Λ-doublet of $Q(3.5)$ transition at 1875.59 cm^{-1} were monitored. The greatest sensitivity was achieved at a modulation amplitude of 140 MHz, corresponding to a modulation index of 2.2 (defined as the ratio of the modulation amplitude to the half width half maximum of the transition), and resulting in a sensitivity of 3.7×10^{-5} cm^{-1} $Hz^{-1/2}$, an enhancement of ca. 23 times on the sensitivity of our direct measurements of the same sample.[32] In this instance, we conducted demodulation of the second harmonic; although the signal amplitude decreases as the harmonic is increased, higher harmonics often lead to flatter baselines — an effect that can be very beneficial, especially when employing multipass cells in which étalon fringing can be a limiting factor on both sensitivity and selectivity. In this manner, WMS has been used to probe OCS within a 20-m White cell and a sensitivity of 1.3×10^{-8} cm^{-1} $Hz^{-1/2}$; clearly, employing a longer-path-length Herriot cell would increase this sensitivity further.[43] Further to the results presented here, greater output power and smaller frequency and intensity instabilities in a newer version of this laser have led to an order of magnitude improvement on our base WMS sensitivity.

4 Summary and Outlook

QCL spectroscopy is already becoming a well-established field of research with many applications already demonstrated. The number of applications will continue to grow in the future as ever cheaper, more reliable, more widely tunable, and short-wavelength devices become available. Even now the production of high-fidelity, short-wavelength devices operating around 3 μm is a rapidly developing field. The QCL, and its sister device the intersubband cascade laser, are thus well placed to be strong contenders for the market currently employing experimentally nontrivial methods such as difference frequency generation and optical parametric oscillators. The combination of high power, broadband tunability, and room-temperature operation promises the extension of optical cavity techniques to the mid-IR, and also further development in the field of trace species detection in a number of environments such as atmospheric monitoring, plasma processing, and breath analysis. Similarly, the next few years will see QCLs further utilized for studies of condensed phases and interfaces. Other applications of such high-powered systems can be found in fundamental studies of chemical dynamics where output powers are now sufficiently high to contemplate using these devices for optical pumping, therefore the preparation of vibrationally excited molecules that are aligned/oriented in the laboratory frame.[44]

Acknowledgments

The authors would like to thank J. Cockburn for the contribution of the 10-μm QCL laser chip. This work is conducted under the Engineering and Physical Sciences Council (EPSRC) program Grant No. EP/G00224X/1: New Horizons in Chemical and Photochemical Dynamics. RJW would like to thank the EPSRC for the award of a postgraduate studentship.

References

1. Y. A. Bakhirkin, A. A. Kosterev, C. Roller, R. F. Curl, and F. K. Tittel, "Mid-infrared quantum cascade laser based off-axis integrated cavity output spectroscopy for biogenic nitric oxide detection," *Appl. Opt.* **43**(11), 2257–2266 (2004).
2. Y. A. Bakhirkin, A. A. Kosterev, R. F. Curl, F. K. Tittel, D. A. Yarekha, L. Hvozdara, M. Giovannini, and J. Faist, "Sub-ppbv nitric oxide concentration measurements using cw thermoelectrically cooled quantum cascade laser-based integrated cavity output spectroscopy," *Appl. Phys. B* **82**(1), 149–154 (2005).
3. G. Duxbury, N. Langford, M. T. McCulloch, and S. Wright, "Quantum cascade semiconductor infrared and far-infrared lasers: from trace gas sensing to non-linear optics," *Chem. Soc. Rev.* **34**, 921–934 (2005).
4. K. Namjou, C. B. Roller, and G. McMillen, "Breath-analysis using mid-infrared unable aser pectroscopy," *Proc. IEEE Sensors* **1–3**, 1337–1340 (2007).
5. R. Provencal, M. Gupta, T. G. Owano, D. S. Baer, K. N. Ricci, and J. R. Podolske, "Cavity-enhanced quantum-cascade laser-based instrument for carbon monoxide measurements," *Appl. Opt.* **44**(31), 6712–6717 (2005).

Downloaded from SPIE Digital Library on 26 Nov 2010 to 130.246.132.178. Terms of Use: http://spiedl.org/terms

6. G. D. Stancu, N. Lang, J. Röpcke, M. Reinicke, A. Steinbach, and A. Wege, "In situ monitoring of silicon plasma etching using a quantum cascade laser arrangement," *Chem. Vapor Deposit.* **13**(6–7), 351–360 (2007).
7. M. L. Silva, A. O'Keefe, D. M. Sonnenfroh, D. I. Rosen, and M. G. Allen, "Integrated cavity output spectroscopy measurements of nitric oxide levels in breath with a pulsed room-temperature quantum cascade laser," *Appl. Phys. B* **81**(5), 705–710 (2005).
8. B. W. M. Moeskops, H. Naus, S. M. Cristescu, and F. J. M. Harren, "Quantum cascade laser-based carbon monoxide detection on a second time scale from human breath," *Appl. Phys. B* **82**(4), 649–654 (2006).
9. D. Weidmann, W. J. Reburn, and K. M. Smith, "Ground-based prototype quantum cascade laser heterodyne radiometer for atmospheric studies," *Rev. of Sci. Instrum.* **78**(7), 073107 (2007).
10. D. Weidmann, W. J. Reburn, and K. M. Smith, "Retrieval of atmospheric ozone profiles from an infrared quantum cascade laser heterodyne radiometer: results and analysis," *Appl. Opt.* **46**(29), 7162–7171 (2007).
11. G. Hancock, S. J. Horrocks, G. A. D. Ritchie, J. H. van Helden, and R. J. Walker, "Time-resolved detection of the CF_3 photofragment using chirped QCL radiation," *J. Phys. Chem. A* **112**(40), 9751–9757 (2008).
12. J. H. van Helden, S. J. Horrocks, and G. A. D. Ritchie, "Application of quantum cascade lasers in studies of low-pressure plasmas: characterization of rapid passage effects on density and temperature measurements," *Appl. Phys. Lett.* **92**(8), 081506 (2008).
13. A. A. Kosterev, F. K. Tittel, C. Gmachl, F. Capasso, D. L. Sivco, J. N. Baillargeon, A. L. Hutchinson, and A. Y. Cho, "Trace-gas detection in ambient air with a thermoelectrically cooled, pulsed quantum-cascade distributed feedback laser," *Appl. Opt.* **39**(36), 6866–6872 (2000).
14. J. H. van Helden, R. Peverall, G. A. D. Ritchie, and R. Walker, "Rapid passage effects in nitrous oxide induced by a chirped external cavity quantum cascade laser," *Appl. Phys. Lett.* **94**(5), 051116 (2009).
15. M. T. McCulloch, G. Duxbury, and N. Langford, "Observation of saturation and rapid passage signals in the 10.25 micron spectrum of ethylene using a frequency chirped quantum cascade laser," *Molec. Phys.* **104**(16), 2767–2779 (2006).
16. G. Duxbury, N. Langford, M. T. McCulloch, and S. Wright, "Rapid passage induced population transfer and coherences in the 8 micron spectrum of nitrous oxide," *Molec. Phys.* **105**(5–7), 741–754 (2007).
17. D. Weidmann, A. A. Kosterev, C. Roller, R. F. Curl, M. P. Fraser, and F. K. Tittel, "Monitoring of ethylene by a pulsed quantum cascadelaser," *Appl. Opt.* **43**(16), 3329–3334 (2004).
18. G. Wysocki, M. McCurdy, S. So, D. Weidmann, C. Roller, R. F. Curl, and F. K. Tittel, "Pulsed quantum-cascade laser-based sensor for trace-gas detection of carbonyl sulfide," *Appl. Opt.* **43**(32), 6040–6046 (2004).
19. L. Allen, and J. H. Eberly, *Optical Resonance and Two-Level Atoms*, Dover, New York (1987).
20. N. Tasinato, G. Duxbury, N. Langford, and K. Hay, "An investigation of collisional processes in a Dicke narrowed transition of water vapor in the 7.8 μm spectral region by frequency down-chirped quantum cascade laser spectroscopy," *J. Chem. Phys.* **132**(4), 044316 (2010).
21. M. Traetteberg, G. Paulen, S. Cyvin, Y. Panchenko, and V. Mochalov, "Structure and confromations of isoprene by vibrational spectroscopy and gas electron-diffraction," *J. Molec. Struct.* **116**(1–2), 141–151 (1984).
22. N. Selamoglu, M. Rossi, and D. Golden, "Absolute rate of recombination of CF_3 radicals," *Chem. Phys. Lett.* **124**(1), 68–72 (1986).
23. N. Basco and F. G. M. Hathorn, "The electronic absorption spectrum of the trifluoromethyl radical," *Chem. Phys. Lett.* **8**(3), 291–293 (1971).
24. A. B. Vakhtin, "The rate constant for the recombination of trifluoromethyl radicals at T = 296 K," *Int. J. Chem. Kinet.* **28**(6), 443–452 (1999).
25. C. E. Brown, J. J. Orlando, J. Reid, and D. R. Smith, "Diode Laser Detection of Transient CF_3 radicals formed by CO_2 laser multiphoton induced dissociation of halocarbons," *Chem. Phys. Lett.* **142**(3–4), 213–216 (1987).
26. G. Wysocki, R. Curl, F. Tittel, R. Maulini, J. Bulliard, and J. Faist, "Widely tunable mode-hop free external cavity quantum cascade laser for high resolution spectroscopic applications," *Appl. Phys. B* **81**(6), 769–777 (2005).
27. L. Hildebrandt, R. Knispel, S. Stry, and J. Sacher, "External cavity QCL systems," *Tech. Messen* **72**(6), 406–412 (2005).
28. M. Beck, D. Hofstetter, T. Aellen, J. Faist, U. Oesterle, M. Ilegems, E. Gini, and H. Melchior, "Continuous wave operation of a mid-infrared semiconductor laser at room temperature," *Science* **295**(5553), 301–305 (2002).
29. G. Wysocki, R. Lewicki, R. F. Curl, H. Q. Le, S. S. Pei, B. Ishaug, and J. Um, "Widely tunable mode-hop free external cavity quantum cascade lasers for high resolution spectroscopy and chemical sensing," *Appl. Phys. B* **92**(3), 305–311 (2008).
30. J. N. Baillargeon, G. P. Luo, C. Peng, H. Q. Le, S. S. Pei, B. Ishaug, and J. Um, "Grating-tuned external-cavity quantum-cascade semiconductor lasers," *Appl. Phys. Lett.* **78**(19), 2834–2836 (2001).
31. A. Hugi, R. Terazzi, Y. Bonetti, A. Wittmann, M. Fischer, M. Beck, J. Faist, and E. Gini, "External cavity quantum cascade laser tunable from 7.6 to 11.4 μm," *Appl. Phys. Lett.* **95**(6), 061103 (2009).
32. G. Hancock, J. H. van Helden, R. Peverall, G. A. D. Ritchie, and R. J. Walker, "Direct and wavelength modulation spectroscopy using a cw external cavity quantum cascade laser," *Appl. Phys. Lett.* **94**(20), 201110 (2009).
33. R. J. Walker, J. H. van Helden, and G. A. D. Ritchie, "Quantum cascade laser absorption spectroscopy of the 1-0 band of deuterium bromide at 5 μm," *Chem. Phy. Lett.* (in press).
34. W. Demtröder, *Laser Spectroscopy: Basic Concepts and Instrumentation*, Springer, Berlin/New York (2003).
35. N. Mukherjee and C. K. N. Patel, "Molecular fine structure and transition dipole moment of NO_2 using an external cavity quantum cascade laser," *Chem. Phys. Lett.* **462**(1–3), 10–13 (2008).
36. J. T. Remillard, D. Uy, W. H. Weber, et al., "Sub-Doppler resolution limited Lamb-dip spectroscopy of NO with a quantum cascade distributed feedback laser," *Opt. Express* **7**(7), 243–248 (2000).
37. S. Bartalini, S. Borri, P. Cancio, et al., "Observing the intrinsic linewidth of a quantum-cascade laser: beyond the Schawlow-Townes limit," *Phys. Rev. Lett.* **104**(8), 083904 (2010).
38. S. Borri, S. Bartalini, I. Galli, et al., "Lamb-dip-locked quantum cascade laser for comb-referenced IR absolute frequency measurements.," *Opt. Express* **16**(15), 11637–11646 (2008).
39. L. S. Rothman, A. Barbe, D. Chris Benner, et al., "The HITRAN molecular spectroscopic database: edition of 2000 including updates through 2001," *J. Quant. Spectrosc. Radiat. Trans.* **82**, 5–44 (2003).
40. M. S. Taubman, T. L. Myers, B. D. Cannon, and R. M. Williams, "Stabilization, injection and control of quantum cascade lasers, and their application to chemical sensing in the infrared," *Spectrochim. Acta, Part A* **60**(14), 3457–3468 (2004).
41. B. A. Paldus, T. G. Spence, R. N. Zare, et al., "Photoacoustic spectroscopy using quantum-cascade lasers," *Opt. Lett.* **24**(3), 178–180 (1999).
42. H. Ganser, W. Urban, and A. M. Brown, "The sensitive detection of NO by Faraday modulation spectroscopy with a quantum cascade laser," *Molec. Phys.* **101**(4–5), 545–550 (2003).
43. L. Ciaffoni, R. Peverall, and G. A. D. Ritchie, "Laser spectroscopy on volatile sulfer compounds:Possibilities for breath analysis," *J. Breath Research* (in press).
44. N. Mukherjee, "Molecular alignment using coherent resonant excitation: a new proposal for stereodynamic control of chemical reactions," *J. Chem. Phys.* **131**(16), 164302 (2009).

Gus Hancock received his first degree from Trinity College Dublin and his PhD degree from Cambridge University. He was a two postdoc with the University of California, San Diego, and was then appointed as Wissenschaftlicher Angestellte in the Universität Bielefeld, Germany. In 1976 he was appointed to a post in physical chemistry at the University of Oxford, where he is now professor of chemistry and heads the Physical and Theoretical Chemistry Laboratory. His awards include the Corday Morgan Medal and Prize, Royal Society of Chemistry in 1982, Royal Society of Chemistry, Reaction Kinetics Award in 1995, the 14th Italgas Prize for Science and Technology for the Environment in 2000, the Polanyi Medal of the Gas Kinetics Group of the Royal Society of Chemistry in 2002, and the Chemical Dynamics Award from the Royal Society of Chemistry in 2010.

Grant Ritchie has worked in the general area of gas phase chemistry for the past 10 years, applying laser techniques to the study of reaction dynamics and trace gas detection. He completed his DPhil degree in 1999 and was awarded a Ramsay Memorial Research Fellowship (2000 to 2003) and then a Royal Society University Research Fellowship (2004 to 2009). Dr. Ritchie has been a lecturer in chemistry at the University of Oxford since 2006. Current research in the Ritchie group is centered on reaction dynamics, optical manipulation, and analytical spectroscopy. In the latter area, their research interests lie in combining diode lasers and quantum cascade lasers with a range of sensitivity enhancing techniques such as modulation spectroscopy and optical-cavity-based absorption methods, for a variety of applications including measurement of trace atmospheric species, probes of the composition of a variety of etching and

Downloaded from SPIE Digital Library on 26 Nov 2010 to 130.246.132.178. Terms of Use: http://spiedl.org/terms

deposition plasmas, and analysis of the contents of human breath and air pollution.

Jean-Pierre van Helden received his MSc degree in applied physics in 2001 and his PhD degree in applied physics in 2006 both from the Eindhoven University of Technology, the Netherlands. In 2007, he joined the Ritchie group at the University of Oxford as a post-doctoral research assistant. He conducts research focused on the development of compact, fast, and ultrasensitive laser-based optical sensors for trace gas detection by means of cavity-enhanced absorption techniques using diode and quantum cascade lasers and their application to atmospheric gas monitoring and diagnostic breath analysis. His current research interest is the application of quantum cascade lasers to problems in nonlinear optics, chemical kinetics, and reaction dynamics.

Richard Walker received his MChem degree from the University of Oxford in 2007 and is currently in his third year reading for his DPhil degree with the Ritchie group. His research is funded by the Engineering and Physical Sciences Council (EPSRC) and is primarily concerned with the application of quantum cascade lasers to spectroscopy, nonlinear optics, and reaction kinetics.

Damien Weidmann graduated in physics in 1998 and earned his PhD degree in applied physics in 2002, both from the University of Reims, France. He subsequently worked as a postdoctoral researcher in the Laser Science Group of Rice University, Houston, Texas. In 2004, he joined the Space Science and Technology Department of the Rutherford Appleton Laboratory, United Kingdom, to initiate, develop, and lead the laser spectroscopy activity within the Spectroscopy Group. Since 2009, he has been with the Physical and Theoretical Chemistry Laboratory through a joint appointment with the University of Oxford, United Kingdom. His research interests are high-resolution tunable laser spectroscopy for remote and *in situ* molecular sensing as well as the development of corresponding instruments and applications.

Downloaded from SPIE Digital Library on 26 Nov 2010 to 130.246.132.178. Terms of Use: http://spiedl.org/terms